Journal of Materials Chemistry A

Accepted Manuscript

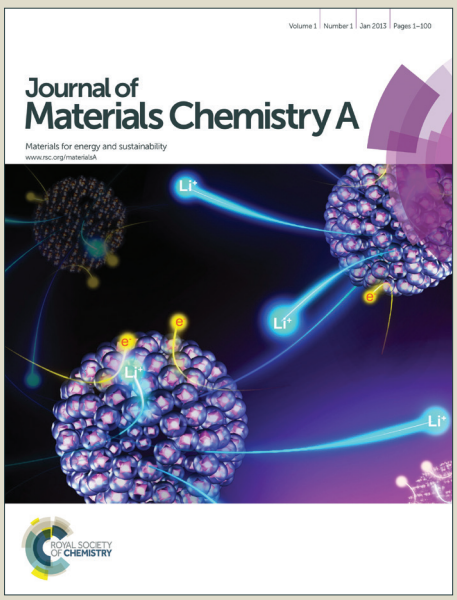

ROYAL SOCIETY OF CHEMISTRY

www.rsc.org/materialsA

Journal Name

ARTICLE

A Green and Facile Method toward Synthesis of Waste Paper-Derived 3 D Functional Porous Graphene via In-Situ Activation of Cobalt (II)

Received 00th January 20xx,
Accepted 00th January 20xx

DOI: 10.1039/x0xx00000x

www.rsc.org/

Dan Xu[a], Yan Xie[b], Yu-Jiang Song[c] and Wei-Qiao Deng[a]*

A cost-efficient and environmental benign strategy for large-scaled production of metal oxide/metal decorated 3D porous graphene directly converted from waste papers with cobalt (II) complex was successfully developed. The resulting Co_3O_4/Co immobilized in porous graphene served as a spacer to prevent restacking of graphene and also provided more accessible active sites. As a demonstration, oxygen reduction reaction (ORR) was chosen to show the catalytic activity of high added-value Co_3O_4/Co @graphene composite. Due to the synergistic catalytic effects between Co_3O_4 and graphene combined with hierarchical porous structure, the synthesized 3D functional porous graphene can function as an efficient ORR catalyst with comparable performance of Pt/C catalyst, which shows its potential application in fuel cells.

1. Introduction

A rising star, graphene, has been attracting more and more attention owing to its unique one atom thick structure and excellent electrical conductivity combined with its extraordinary mechanical strength.[1] Promising applications have been developed such as gas separation, catalysis, water purification, energy conversion and storage.[2] Accordingly, extensive efforts have been made at the preparation of graphene with various physical forms from diverse sources to fit the desired applications.[3] Furthermore, with the aim of bringing graphene from the laboratory into market, low value sources are favored. Among them, organic waste matter is ideal carbon source for preparing graphene due to its abundance, low cost, and easy to obtain. Thereby, a strategy based on organic waste matter to easily, efficiently, and sustainably accessible various functional graphene at large scale is highly desirable.

Waste paper is the major source of organic wastes.[4] The main components of paper are carbohydrate, such as cellulose and hemicelluloses, and some lignin, indicating that waste paper could act as an ideal carbon source to high added-value graphene. Although amorphous carbon materials with various fascinating structures derived from organic waste matter have exhibited significant promising applications[5] and model sugar compounds or small molecules as carbon source for graphene production have been reported,[6] only few papers have reported high added-value functional graphene production from organic waste.[7] Moreover, these typical methods need special substrate and template combined with tedious processes. In addition, extra strong chemical activation step was used for porous system.

Herein we introduced a cost-efficient and environmental benign strategy for large scale production of metal oxide

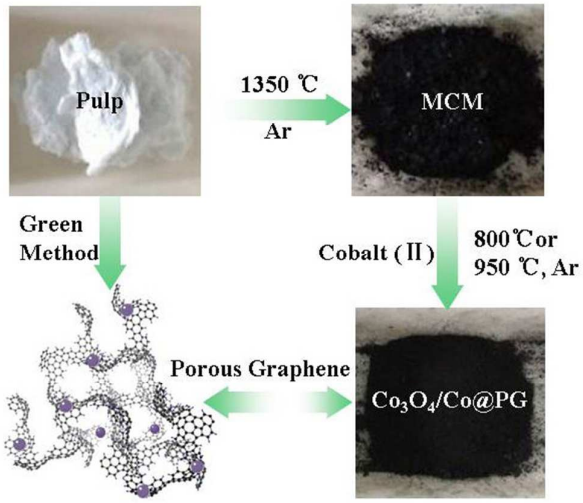

Scheme 1 Schematic procedure for functional porous graphene (Co_3O_4/Co@PG) from waste paper (MCM stands for microporous carbonaceous material and PG stands for porous graphene).

[a] State Key Lab of Molecular Reaction Dynamics, Dalian National Laboratory for Clean Energy, Dalian Institute of Chemical Physics, Chinese Academy of Sciences , Dalian, 116023, China. E-mail: dengwq@dicp.ac.cn..
[b] Center of Gold Catalysis, Dalian Institute of Chemical Physics, Chinese Academy of Sciences, Dalian 116023, China..
[c] State Key Laboratory of Fine Chemicals, School of Chemical Engineering, Dalian University of Technology, 116024, China..
Electronic Supplementary Information (ESI) available. See
DOI: 10.1039/x0xx00000x

/metal decorated 3D porous graphene, in which the waste paper was used as carbon source. In addition, cobalt(II) acetate- 1,10-phenanthroline complex acted as a precursor of both catalyst and etcher. Through control of the feed ratio of organometallic complexes and pyrolysis temperature, the porosity of graphene supporter and chemical compositions of active sites could be finely tuned. The synthesized 3D functional porous graphene is an ideal material beneficial in electrochemistry catalytic areas that require excellent electrical conductivity, high specific surface area, and easier accessibility to the active sites through porous system.[8] As a demonstration, this material exhibited excellent catalytic efficiency for oxygen reduction reaction (ORR) with comparable performance to Pt/C catalyst.

2. Experimental section

2.1 Chemicals

Carbon source was waste office paper (A4 size, out dated printed files). Cobalt(II) acetate anhydrous was purchased from Alfa Aesar. 1,10-phenanthroline was brought from J&K. Meso-tetraphenylporphyrin was obtained from Frontier Scientific Inc. Anhydrous ethanol and other affiliated chemicals were all from local suppliers. All solvents and chemicals were of reagent quality and were used without further purification.

2.2 Synthesis of functional porous graphene

Preparation of carbonaceous pulp: Waste office paper was first treated with HCl (10 wt%) for hydrolysis for 72 h and was washed with large amount of distilled water to completely remove chloride ions. After that, the pulp was dispersed in distilled water with vigorous stirring for 12 h and then was dried in oven at 80 °C for 6 h. The first step for pulp graphitization was carried out at 1350 °C for 3 h with heating rate of 4 °C per minute under argon atmosphere. The obtained microporous carbonaceous pulp at a yield of 8% was labeled as MCM.

Co_3O_4@Graphene: MCM (138 mg) was added to a solution of cobalt (II) acetate (0.1 mmol, 0.0177 g) and 1,10-phenanthroline (0.2 mmol, 0.036 g) complex in 10 ml ethanol by sonication for 1 h to achieve uniform dispersion. After removal of ethanol in vacuum, the resulting solid sample was heated to 800 °C for 2 h at the rate of 4 °C per minute under argon atmosphere (20% yield). No ligand@PG (without ligand) and Porphyrin@PG (Meso-tetraphenylporphyrin (0.1 mmol, 0.0194 g)) were performed under the same condition.[9]

Co@Graphene: MCM (138 mg) was added to a solution of cobalt (II) acetate (1mmol, 0.177g) and 1,10-phenanthroline (2 mmol, 0.36 g) complex in 20 ml ethanol by sonication for 1 h to achieve uniform dispersion. After removal of ethanol in vacuum, the resulting solid sample was heated to 950 °C for 1 h at the rate of 4 °C per minute under argon atmosphere (10% yield).[10]

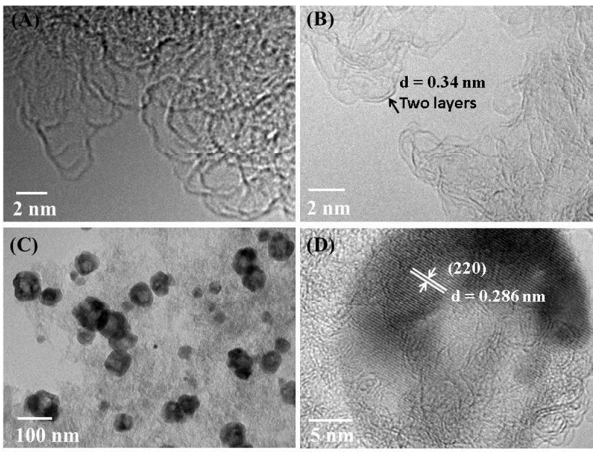

Fig. 1 HRTEM images of carbonaceous pulp (A), edge of Co_3O_4@PG (B), Co_3O_4@PG hybrid (C), and Co_3O_4 nanoparticle in graphene (D).

2.3 Electrochemical test

Electrocatalytic activity of as-prepared samples in 0.1 M KOH were tested on a CHI 760D electrochemical working station (CH Instruments, Shanghai, China). The working electrode was prepared under the guidance of procedure described in Ref. 11.

The graphene catalyst ink was prepared to be 2 mg/mL in a solution of ultrapure water, ethanol, and Nafion solution (5wt%, Dupont) (volume ratio =1: 9: 0.1) followed by strong ultrasonic agitation. In a typical test, 60 µL of the graphene ink was pasted onto the glassy carbon rotating disk electrode (RDE) (5 mm in diameter, 0.19625 cm^2, Pine Instruments, USA), with a sample loading of 0.6 mg cm^{-2}. For comparison, 5 µL of commercial Pt/C (20 wt% Pt/C, Johnson Matthey) of 1 mg/mL was loaded on RDE using the same procedure with a loading of 5 $\mu g_{Pt} cm^{-2}$.[11]

All the measurements were performed using Pt mesh as the counter electrode and Hg/HgO as the reference electrode. Cyclic voltammetry (CV) curves were carried out in both N_2 and O_2 saturated 0.1 M KOH solution at a scan rate of 100 mV/s. ORR polarization curves were detected in the O_2-satureated solution (0.1 M KOH) at a positive scan rate of 5 mV/s from -0.8 to 0.2 V at 1600 rpm. ORR polarization curves were measured with RDE from the rotating speeds of 400 rpm to 2500 rpm at 5 mV/s.

3. Results and discussion

The production of 3D functional porous graphene from waste paper needs 3 steps (Scheme 1): hydrolysis,[12] carbonization, and carbothermal reaction[13]. Finally, waste paper-derived and Co_3O_4/Co decorated porous graphene was successfully prepared at 800 °C and 950°C, respectively (labeled as Co_3O_4/Co@PG).

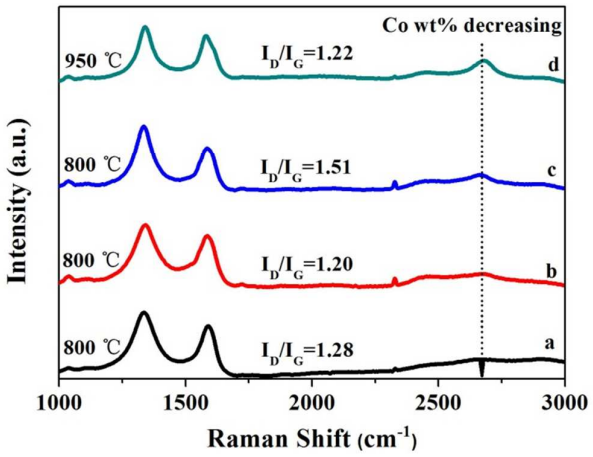

Fig. 2 Raman spectra of MCM (a), TPG (b), Co_3O_4@PG (c), and Co@PG (d).

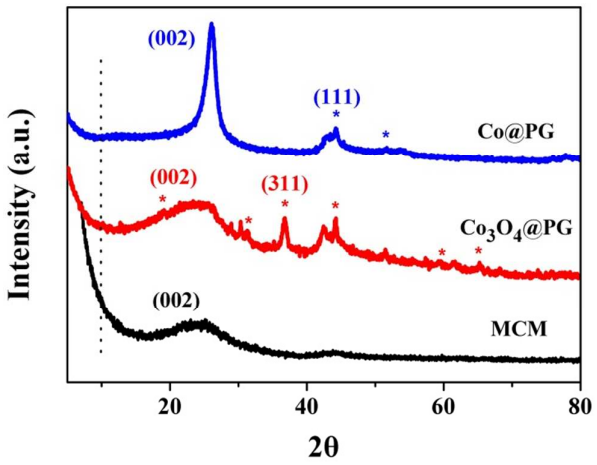

Fig. 3 XRD pattern of MCM (a), Co_3O_4@PG (b), and Co@PG (c).

The morphology of the waste paper-derived graphene and the composition of the forming particle were investigated by SEM, HRTEM, Raman, XRD, and XPS. The particle size with wide size distribution increased from 50 nm-100 nm to 200 nm cluster with the increasing amount of organometallic complexes loaded (Fig. S1A, Fig. S1C). SEM images also showed that some pores formed because the carbon atom reacted with the metal oxide nanoparticles (Fig. S1B, Fig. S1D). Both SEM and HRTEM images (Fig. 1C, 1D, Fig. S2B, and 2C) indicated that particles were distributed in and on the resulting material. From HRTEM image it can be seen that the graphene layer became thinner compared with the graphitized pulp because of the effect of etcher (Fig. 1A, Fig. 1B, and Fig. S2A). Typical Raman spectra are more informative to show the quality of graphene. Three prominent features of graphene, the D peak, G peak, and 2D peak appeared after the graphitized pulp was activated by cobalt(II) acetate- 1,10-phenanthroline (Fig. 2b ,c, d).[14] D-band (at 1338 cm^{-1}) reflects disordered carbon (sp^3), G peak (at 1586 cm^{-1}) is characteristic of sp^2 hybridization, and 2D peak is the overtone of D peak. I_{2D}/I_G (intensity ratio between 2D and G peak) combined with the full width half maximum (FWHM) of the 2D peak are very critical to evaluate the number of graphene layers. For all the activated materials, I_{2D}/I_G value is lower than 0.75 and W_{2D} value is higher than 65 cm^{-1},[15] indicating that multi-layer graphene were obtained from waste paper. Because gaphene oxide has a strong diffraction peak at about 2θ=10° with a d-spacing of 1 nm in XRD spectra, Figure 3 indicates that the obtained sample does not have graphene oxide (no peak around 2θ=10°).[16] Furthermore, selected double-layer region was marked with a layer-to-layer stacking distance of 0.34 nm (Fig. 1B) for graphite also demonstrating that the carbon material is graphene.[17] The I_D/I_G (intensity ratio between D and G peak) is widely used to assess the quality of graphene. With a 0.02 wt% loading of cobalt (II) (labeled as TPG), the ratio of I_D/I_G slightly decreased compared with originally graphitized pulp at annealing temperature of 800 °C. It may attribute to the preferential etching of more reactive amorphous carbon components.[18] To further increase the loading of cobalt (II) (0.5 wt%), the ratio of I_D/I_G increased from 1.20 to 1.51 indicating that more defects or disorder appeared due to further carbothermal reaction between in situ formed metal oxide and carbon atoms. However, the ratio of I_D/I_G decreased from 1.51 to 1.22 with both the loading of cobalt (II) (2 wt%) and annealing temperature increasing (950 °C) at the same time. These values are lower than porous graphene microspheres (an I_D/I_G ratio of 1.96), but are higher than Ni-decorated graphene (an I_D/I_G ratio of 0.5)[7d] and sugar derived graphene (an I_D/I_G ratio of 1.07).[19]

The final active species were different. Energy dispersive X-ray (EDX) analysis preliminary indicated that the formed particle was Co_3O_4 (Fig. S1E) at an annealing temperature of 800 °C and Co at 950 °C (Fig. S1F). The obtained samples were labeled as Co_3O_4@PG and Co@PG, respectively (Table S1). In Fig. 3, the strongest peak located at 36.8° of Co_3O_4@PG corresponds to the Co_3O_4 (311) plane[20] and (111) plane at 44.3° of Co@PG indicated the formation of Co metal particles.[21] Lattice fringes of 0.286 nm and 0.24 nm corresponding to the Co_3O_4 (220) plane and CoO (111) plane in Fig. 1D and Fig. S2D respectively further confirmed the existence of Co_3O_4 and Co.[22] X-ray photoelectron spectroscopy (XPS) showed the main component of the composite (Fig. 4A, and Table S2) and high resolution XPS spectra further confirmed the chemical compositions of active sites. A doublet bands appeared at 778.9 eV and 794.5 eV was attributed to Co_3O_4 (Fig. 4B a).[23] For cobalt metal, the low energy band of Co $2p_{3/2}$ located at 777.2 eV (Fig. 4B b).[24] Furthermore, the morphology and microstructure of graphene also changed because of the effect of etcher. The diffraction peaks appeared at 23.5°, 24.0°, and 26.3° were (002) plane of graphite, corresponding to MCM, Co_3O_4@PG, and Co@PG, respectively. The diffraction peak shifted to a higher angle with defect density increased indicating that the spacing between the layers of Co_3O_4@PG was reduced. In contrast, interlayer *d*- spacing of 0.336 nm as that of graphite and the decreased value of I_D/I_G of Co@PG exhibited the improved graphitization degree.[25] The possible reason was that more disordered carbon (sp^3) could be etched with the increase of loading amount of cobalt (II) (from 0.5 to 2

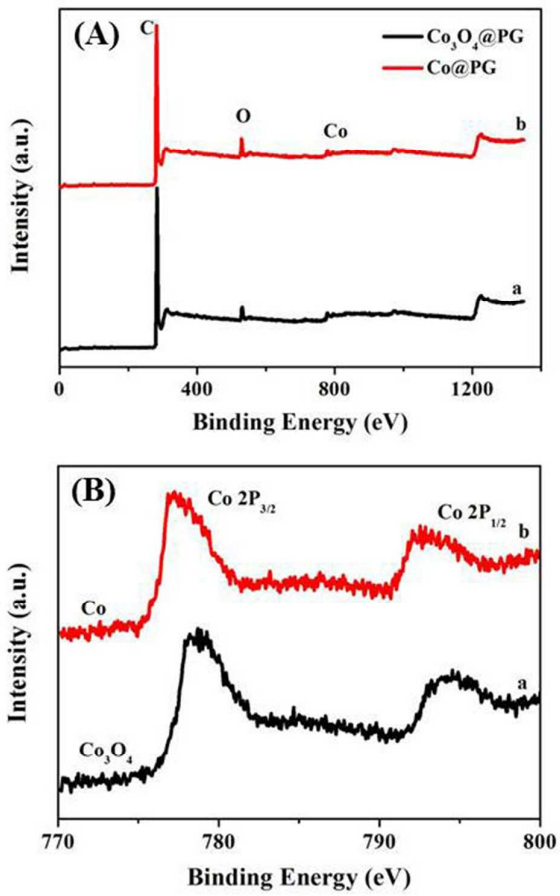

Fig. 4 X-ray photoelectron spectroscopy (XPS) spectrum of Co_3O_4@PG (a) and Co@PG (b) (A); Co 2p spectrum of Co_3O_4@PG (a) and Co@PG (b) (B).

wt%). Furthermore, the Brunauer–Emmett–Teller (BET) surface area of Co_3O_4@PG was 542 m^2/g which is higher than that of Co_3O_4 nanoparticles anchored reduced graphene oxides (139.4 m^2/g).[26] The main pore size of Co_3O_4@PG distributed at 0.4 nm and 4 nm. While for Co@PG, a clear hysteresis loop appeared in the isotherm with BET surface area of 186 m^2/g illustrating the existence of mesopores and this was further confirmed by pore size distribution analysis (18-20 nm) attributing to the effect of the in situ formed etcher (Fig. S3 and Fig. S4). The total pore volumes of Co_3O_4@PG and Co@PG were 0.34 and 0.15 cm^3/g, respectively. Based on sugar-blowing approach, pore size distribution of the prepared graphene ranged from 4-30 nm[6b] and graphene grown by CVD possessed pores in the mesopore region (2–7 nm) with total pore volume of 2 cm^3/g.[17] In this work, through the optimization of the concentration of the precursor and pyrolysis temperature, we successfully tailored the active components as well as pore size distribution (0.4-20 nm) of functional porous graphene via a green and facile way.

For the first step, because of the similar main components of paper, such as cellulose and hemicelluloses, and some lignin, waste paper could act as an ideal carbon source to high added-value materials. In fact, various forms of waste paper have been employed as the raw material for producing functional carbon materials, such as disposable paper cups,[7b] waste office papers,[12, 5b] and waste newspapers.[27] In this work, the waste office papers were selected as carbon source and other waste papers should function in similiar way as well.

The use of HCl for hydrolysis is a step with low cost, because HCl is basic industrial chemical and also basic chemical in lab. The high-temperature treatment may cost more, but it is a necessary step for the fabrication of most porous carbons. For example, preparation of waste paper derived carbon microbelt aerogel was pyrolyzed at 850 °C.[12] Graphene sheets prepared from disposable paper cups was heated at 1100 °C.[7b] Sugar derived 3D graphene bubble network was treated at 1,350 °C.[6b]

For the second step, pulp carbonization was different from small molecule polymerization because of its relatively complex composition and structure. To make pulp well-graphitized, a higher pyrolysis temperature 1350 °C was used. With such temperature the degree of graphitic order can be improved and oxygen and hydrogen tend to loss from the carbonaceous pulp.[28] Nitrogen sorption analysis was also performed to the carbonaceous pulp displaying a Type I isotherm with BET surface area of 1050 m^2/g, main micropore-size of 0.5 nm and wide size distribution of mesopore (Fig. S3 and Fig. S4). Low-magnification SEM image (Fig. S5A) showed that the pyrolyzed carbonaceous pulp showed belt-like structure. Wrinkles, concaves, and flexible thin layer appeared in high-magnification SEM images (Fig. S5B, C, and D). Obvious aggregation and sparse thin layers could be observed in HRTEM (Fig. 1A).

For the third step, it was reported that the concentration of the precursor is a key parameter determining the metal oxide particle size and the following pore size of the substrate.[13] Herein, cobalt (II) acetate- 1,10-phenanthroline complex served as precursor of both etcher and catalyst. The organometallic complexes first transformed into metal oxide particles as the etcher and then through a carbothermal reaction converted to final active catalyst in the form of Co_3O_4 or Co particles impregnated in porous graphene. The two processes controlled the structure of the graphitized pulp and further determined the electrocatalytic activity of the resulting material.

Due to the excellent electrical conductivity, high specific surface area, and easier accessibility to the active sites, ORR was employed as a model reaction to evaluate catalytic activity of the Co_3O_4@PG and Co@PG composites. Cyclic voltammetry (CV) was first performed on the as-prepared samples. CV curves in Fig. 5A of Co_3O_4@PG showed an apparent reductionpeak in the O_2-saturated 0.1 M KOH electrolyte; whereas no electrochemical response appeared under nitrogen indicating that the electrocatalytic activity of the sample was caused by the reduction of oxygen. To further test the electrocatalytic activity of the two samples, the rotating disk electrode (RDE) measurements in O_2 saturated electrolyte (0.1 M KOH) at a scanning rate of 5mV/s was also performed to investigate the reaction kinetics and20 wt% Pt/C (Johnson Matthey) as well as the TPG were also tested for comparison.

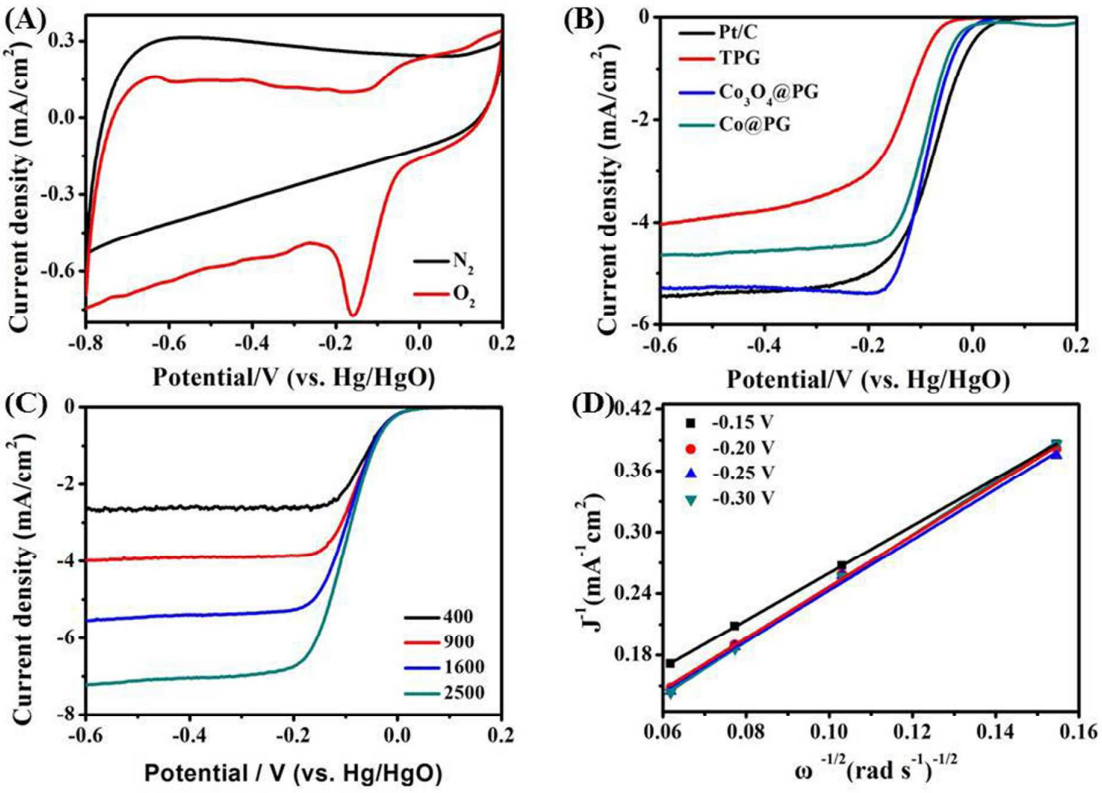

Fig. 5 (A) CV curve of Co_3O_4@PG in N_2 (Black)- and O_2 (Red)-saturated 0.1 M KOH; (B) ORR polarization curves of PG, Co_3O_4@PG, Co@PG, and commercial Pt/C catalysts in O_2-saturated 0.1 M KOH with a scanning rate of 5 mV s^{-1} at 1600 rpm; (C) ORR polarization curves of Co_3O_4@PG in O_2-saturated 0.1 M KOH with a scanning rate of 5 mV s^{-1} at various rotation rates (400-2500 rpm); (D) K-L plots at different potentials from -0.15 to -0.30 V based on the data from (C).

ORR polarization curves of Co_3O_4@PG showed enhanced ORR catalytic activity than Co@PG with a 12 mV positive onset potential (E_{onset}) and a 4 mV positive half-wave potential ($E_{1/2}$), and TPG showed less ORR catalytic activity. Furthermore, the ORR activity and limiting current density of Co_3O_4@PG was comparable to that of Pt/C (5 μg-$_{Pt}$cm^{-2}) (Fig. 5B). This could be attributed to catalytical activity of Co_3O_4 at the interface of porous graphene in ORR.[29] We chose Pt/C with the platinum loading 5 μg cm^{-2} because it has similar metal loading as the Co_3O_4@Graphene (0.6 mg cm^{-2}) in which the cobalt loading was 3 μg cm^{-2}. Cobalt is one of the most promising non-platinum-group-metal catalysts for the ORR.[31] Co_3O_4@Graphene with a loading of 3 μg-$_{Co}$cm^{-2} showed comparable performance to Pt/C catalyst with a loading of 5 μg-$_{Pt}$cm^{-2} demonstrating high catalytic activity of high added-value Co_3O_4@graphene composite.

Fig. 5C showed the ORR polarization curve of Co_3O_4@PG at different rotation speeds from 400 to 2500 rpm. Koutecky-Levich (K-L) plots (J^{-1} versus $\omega^{-1/2}$) at reaction potentials from -0.3 to 0.1 V was used to further evaluate catalytic performance of Co_3O_4@graphene (Fig. 5D). The good linear relations in K-L plots and slightly changed slopes of the fitting lines over the potentials of selected region indicated the similar number of transferred electron for the ORR. The average electron transfer number (n) was calculated based on slopes of 3.5–3.9, exhibiting a direct 4-electron reduction process of O_2 to H_2O.[11] Based on CV and ORR curves measurements, it is evident that Co_3O_4 decorated porous graphene derived from waste paper showed high catalytic activity in ORR.

Organic ligands have potential effect on precatalyst.[9] To obtain further insight into the role of organic ligand, $Co(OAc)_2$ and $Co(OAc)_2$-tetraphenylporphrin as precursor loaded on MCM (labeled as No ligand@PG and Porphyrin@PG) were carried out on RDE measurements (Fig. S6). ORR polarization curve of No ligand@PG showed less ORR catalytic activity than Co_3O_4@PG, with a 21 mV negative E_{onset} and a 30 mV negative $E_{1/2}$. Porphyrin@PG also showed less catalytic activity in ORR. The comparative experimental results clearly indicated that organic ligand is the key to determine the final electrocatalytic activity. In addition, EC-600, another kind of commercially available carbon was selected as a supporter for comparison for ORR. Poor catalytic activity was observed (Fig. S6). The results described in our work demonstrated enhanced ORR catalytic activity of Co_3O_4@PG as electrocatalyst. One of the purposes using graphene is to disperse Co_3O_4 or Co nanoparticles and serve as a current conductor. Another purpose is the synergistic coupling mechanism between Co_3O_4 and graphene, because Co_3O_4 and CMC alone have little

catalytic activity. At the same time, Co_3O_4@EC600 also showed poor catalytic activity, which was similar to the reference 29b report by Dai et al. In fact, Co_3O_4@graphene and Co/CoO@graphene have been extensively used for electrochemical reduction of oxygen where graphene functioned as supporter. In this work, Co_3O_4/Co particles were in situ deposited in and on the surface of graphene with tight contact existing charge-transfer interactions.[30] Xiao et al. have found that Co^{2+} in Co_3O_4 ($Co^{2+}Co^{3+}{}_2O_4$) acted as the catalytically active sites instead of Co^{3+} sites for ORR.[26] For Co@PG, because of the oxidization of metal cobalt to CoO in air at room temperature, nearly 1 nm thick layer of CoO played the key role for ORR.[32] Therefore, excellent electrical conductivity of graphene, the synergistic catalytic effects between Co_3O_4 and graphene, and hierarchical porous structure for efficient mass transport contributed to the enhanced catalytic activity of Co_3O_4@PG.

A method that can synthesize functional graphene with active components in economically beneficial and environmental benign ways is the most important for large scale application of graphene. Aforementioned results clearly showed that high added-value 3D functional porous graphene with electrochemical catalytic activity can be simply prepared from waste paper. The functional graphene has comparable activity to Pd/C for oxygen reduction reaction. These results also demonstrated that by prudently screening of ligand, metal, and the optimization of the preparation conditions, it is possible to produce multi-functional porous graphene with application range widely from catalyst to sensor and microwave absorption.

4. Conclusions

In conclusion, a green, facile and efficient strategy for large scale production of functional porous graphene from waste paper by in-situ activation of Co (II)-Amine complex was demonstrated. The complex served as precursor of both catalyst and etcher. The as-prepared Co_3O_4@PG composite showed high-performance catalytic activity in ORR. Hence, this green method provides guidance for efficiently design of multi-functional porous graphene.

Acknowledgements

We gratefully acknowledge financial support from the National Science Foundation of China (21373202, 91333116, 21173209) and China Postdoctoral Science Foundation (2013M530950).

Notes and references

1 (a) L. Jiang and Z. Fan, *Nanoscale*, 2014, **6**, 1922; (b) X. Wang and G. Shi, *Energy Environ. Sci*., 2015, **8**, 790.

2 (a) X. Zhu, C. Tian, S. Chai, K. Nelson, K. S. Han, E. W. Hagaman, G. M. Veith, S. M. Mahurin, H. Liu and S. Dai, *Adv. Mater*., 2013, **25**, 4152; (b) C. Tang, Q. Zhang, M. Zhao, J. Huang, X. Cheng ,G. Tian , H. Peng and, F. Wei, *Adv. Mater*., 2014, **26**, 6100; (c) R. Raccichini, A. Varzi, S. Passerini and B. Scrosati, *Nat. Mater*., 2015, **14**, 271; (d) R. K. Joshi, P. Carbone, F. C. Wang, V. G. Kravets, Y. Su, I. V. Grigorieva, H. A. Wu, A. K. Geim and R. R. Nair, *Science*, 2014, **343**, 752; (e) J. Ahn, B. H. Hong, F. Torrisi, J. N. Coleman, J. Liu, S. Böhm, M. Drndić, K. Kostarelos, K. S. Novoselov and E. J. Siochi, *Nature Nanotech*, 2014, **9**, 737; (f) L. Gao, L. Li, X. Wang, P. Wu, Y. Cao, B. Liang, X. Li, Y. Lin, Y. Lu and X. Guo. *Chem. Sci*., 2015, **6**, 2469.

3 (a) A. Narita, X. Feng, Y. Hernandez, S. A. Jensen, M. Bonn, H. Yang, I. A. Verzhbitskiy, C. Casiraghi, M. R. Hansen, A. H. R. Koch, G. Fytas, O. Ivasenko, B. Li, K. S. Mali, T. Balandina, S. Mahesh, S. D. Feyter and K. Müllen, *Nat. Chem*., 2014, **6**, 126; (b) K. R. Paton et al. *Nat. Mater*., 2014,**13**, 624; (c) M. Wang, S. K. Jang, W. Jang, M. Kim, S. Park, S. Kim, S. Kahng, J. Choi, R. S. Ruoff, Y. J. Song and S. Lee, *Adv. Mater*., 2013, **25**, 2746; (d) Y. Zhao, C. Hu, Y. Hu, H. Cheng, G. Shi and L. Qu, *Angew. Chem. Int. Ed*., 2012, **51**, 11371; (e) M. Titirici, R. J. White, N. Brun and V. L. Budarin, *Chem. Soc. Rev*., 2015, **44**, 250; (f) M. Yi and Z. Shen, *J. Mater. Chem. A*, 2015, **3**, 11700.

4 (a) L. Wang, M. Sharifzadeh, R. Templer and R. J. Murphy, *Energy Environ. Sci*., 2012, **5**, 5717; (b) L. Wang, R. Templer and R. J. Murphy, *Energy Environ. Sci*., 2012, **5**, 8281.

5 (a) M. Biswal, A. Banerjee, M. Deo and S. Ogale, *Energy Environ. Sci*., 2013, **6**, 1249; (b) D. Puthusseri, V. Aravindan, B. Anothumakkool, S. Kurungot, S. Madhavi and S. Ogale, *Small*, 2014, **10**, 4395; (c) Y. S.Yun , S. Y. Cho , J. Shim , B. H. Kim , S. Chang ,S. J. Baek , Y. S. Huh , Y. Tak , Y. W. Park , S. Park and H. Jin, *Adv. Mater*., 2013, **25**, 1993; (d) W. Qian, F. Sun, Y. Xu, L. Qiu, C. Liu, S. Wang and F. Yan, *Energy Environ. Sci*., 2014, **7,** 379.

6 (a) Y. Fang, Y. Lv, R. Che, H. Wu, X. Zhang, D. Gu and G. Zheng, *J. Am. Chem. Soc*., 2013, **135**, 1524; (b) X. Wang, Y. Zhang, C. Zhi, X. Wang, D. Tang, Y. Xu, Q. Weng, X. Jiang, M. Mitome, D. Golberg and Y. Bando, *Nat. Commun*., 2013, **4**, 2905; (c) X. Liu and M. Antonietti, *Adv. Mater*., 2013, **25**, 6284.

7 (a) G. Ruan, Z. Sun, Z. Peng and J. M. Tour, *ACS Nano*, 2011, **5**, 7601; (b) H. Zhao and T. S. Zhao, *J. Mater. Chem. A*, 2013, **1**, 183; (c) O. Akhavan, K. Bijanzad and A. Mirsepah, *RSC Adv*., 2014, **4**, 20441; (d) A. K. Ray, R. K. Sahu, V. Rajinikanth, H. Bapari, M. Ghosh and P. Paul, *Carbon*, 2012, **50**, 4123; (e) D. H. Seo, A. E. Rider, Z. J. Han, S. Kumar and K. Ostrikov. *Adv. Mater*., 2013, **25**, 5638; (f) K. H. Adolfsson, S. Hassanzadeh and M. Hakkarainen, *RSC Adv*., 2015, **5**, 26550.

8 (a) H. Tang, H. Yin, J. Wang, N. Yang, D. Wang, and Z. Tang, *Angew. Chem. Int. Ed*., 2013, **52**, 5585; (b) X. Zhou, Z. Bai, M. Wu, J. Qiao and Z. Chen, *J. Mater. Chem. A*, 2015, **3**, 3343; (c) Q. Dong, X. Zhuang, Z. Li, B. Li, B. Fang, C. Yang, H. Xie, F. Zhang and X. Feng, *J. Mater. Chem. A*, 2015, **3**, 7767.

9 F. A. Westerhaus, R. V. Jagadeesh, G. Wienhöfer, M. Pohl, J. Radnik, A. Surkus, J. Rabeah, K. Junge, H. Junge, M. Nielsen, A. Brückner and M. Beller, *Nat. Chem*., 2013, **5**, 537.

10 H. T. Chung, J. H. Won and P. Zelenay, *Nat. Commun*., 2013, **4**, 1922

11 Y. Xie, C. Tang, Z. Hao, Y. Lv, R. Yang, X. Wei, W. Deng, A. Wang, B. Yi and Y. J. Song, *Faraday Discuss*., 2014, **176**, 393.

12 H. Bi , X. Huang , X. Wu , X. Cao , C. Tan , Z. Yin , X. Lu , L. Sun and H. Zhang, *Small*, 2014, **10**, 3544.

13 D. Zhou, Y. Cui, P. Xiao, M. Jiang and B. Han, *Nat. Commun*., 2014, **5**, 4716.

14 A. C. Ferrari and D. M. Basko, *Nature Nanotech*., 2013, **8**, 235.

15 (a) Y. Gong, X. Zhang , G. Liu, L. Wu, X. Geng, M. Long, X. Cao, Y. Guo, W. Li, J. Xu, M. Sun, L. Lu and L. Liu, *Adv. Funct. Mater*., 2012, **22**, 3153; (b) Y. Ito, Y. Tanabe, H. Qiu, K. Sugawara, S. Heguri, N. H. Tu, K. K. Huynh, T. Fujita, T. Takahashi, K. Tanigaki and M. Chen, *Angew. Chem. Int. Ed*., 2014, **53**, 4822.

16 S. Mao, H. Pu and J. Chen*, RSC Adv*., 2012, **2**, 2643; b) C. Tao, J. Wang, S. Qin, Y. Lv, Y. Long, H. Zhua and Z. Jiang, *J. Mater. Chem*., 2012, **22**, 24856.
17 M. Q. Zhao, Q. Zhang, J. Q. Huang, G. L. Tian, J. Q, Nie, H. J. Peng and F. Wei, *Nat. Commun*., **5**, 3410.
18 J. Biener, S. Dasgupta, L. Shao, D. Wang, M. A. Worsley, A. Wittstock, J. R. I. Lee, M. M. Biener, C. A. Orme, S. O. Kucheyev, B. C. Wood, T. M. Willey, A. V. Hamza , J. Weissmüller, H. Hahn and T. F. Baumann, *Adv. Mater*., 2012, **24**, 5083.
19 J. L. Shi, H. J. Peng, L. Zhu, W. Zhu and Q. Zhang, *Carbon*, 2015, **92**, 96; b) F. Pan, J. Jin, X. Fu, Q. Liu and J. Zhang. *ACS Appl. Mater. Interfaces*, 2013, **5**, 11108.
20 Z. Wu, W. Ren, L. Wen, L. Gao, J. Zhao, Z. Chen, G. Zhou, F. Li and H. Cheng, *ACS Nano*, 2010, **4**, 3187.
21 T. M. Keller, S. B. Qadrib and C. A. Little, *J. Mater. Chem*., 2004, **14**, 3063.
22 H. Lv, X. Liang, G. Ji, H. Zhang and Y. Du, *ACS Appl. Mater. Interfaces*, 2015, **7**, 9776.
23 L. Fu, Z. Liu, Y. Liu, B. Han, P, Hu, L. Cao and D. Zhu. *Adv. Mater*., 2005, **17**, 217.
24 R. Riva, H. Miessner, R. Vitali and G. D. Piero. *Appl. Catal. A-Gen*., 2000, **196**, 111.
25 K. Parvez, Z. Wu, R. Li, X. Liu, R. Graf, X. Feng and K. Müllen, *J. Am. Chem. Soc*., 2014, **136**, 6083.
26 J. Xiao, Q. Kuang, S. Yang, F. Xiao, S. Wang and L. Guo, *Scientific Reports,* 2013, **3**, 2300
27 D. Kalpana, S. H. Cho, S. B. Lee, Y. S. Lee, R. Misra, N. G. Renganathan, *J. Power Sources*, 2009, **190**, 587.
28 T. Fellinger, R. J. White, M. Titirici and M. Antonietti, *Adv. Funct. Mater*., 2012, **22**, 3254.
29 (a) S. Mao, Z. Wen, T. Huang, Y. Houa, J. Chen, *Energy Environ. Sci*., 2014, **7**, 609; (b) Y. Liang, Y. Li, H. Wang, J. Zhou, J. Wang, T. Regier and H. Dai, *Nat. Mater*., 2011, **10**, 780.
30 S. Guo, S. Sun, *J. Am. Chem. Soc*., 2012, **134**, 2492.
31 F. Jaouen, E. Proietti, M. Lefèvre, R. Chenitz, J. Dodelet, G. Wu, H. T. Chung, C. M. Johnstonb and P. Zelenay, *Energy Environ. Sci.,* 2011, **4,** 114
32 S. Guo, S. Zhang, L. Wu, and S. Sun, *Angew. Chem. Int. Ed*., 2012, **51**, 11770.

Graphical abstract:

Using waste paper as carbon source, a strategy for efficient production of Co_3O_4/Co@porous graphene for oxygen reduction reaction was developed, which provides a direction for facile preparation of functional porous graphene from wastes.